Mechanics of Advanced Composite Structures

On Moving Harmonic Load and Dynamic Response of Carbon Nanotube-Reinforced Composite Beams using Higher-Order Shear Deformation Theories

M. Eghbali [a] ⓘD, S.A. Hosseini [b]* ⓘD

[a] Department of Mechanical Engineering, University of Zanjan, Zanjan, Iran
[b] Department of Industrial, Mechanical and Aerospace Engineering, Buein Zahra Technical University, Qazvin, Iran

KEYWORDS

ABSTRACT

This paper uses different higher-order shear deformation theories to analyze the axial and transverse dynamic response of carbon nanotube-reinforced composite (CNTRC) beams under moving harmonic load. The governing equations of the CNTRC beam are obtained based on the shear deformation beam theory and the Hamilton principle. The exact solution for dynamic response is presented using the Laplace transform. A comparison of previous studies has been published, where a good agreement is observed. Finally, some examples were used to analyze aspect ratio, other higher-order theories, excitation frequency, the volume fraction of Carbon nanotubes (CNTs), the velocity of a moving harmonic load, and their influence on axial and transverse dynamic and maximum deflections. It was observed that the X-beam is a stronger beam than other CNT patterns, Reddy theory is the lower limit, and HSDT theory is the upper limit. The vibration response and dynamic movement of the structure can be controlled by choosing the appropriate items.

1. Introduction

The mechanical, thermal, and electrical properties of carbon nanotubes (CNTs) make them suitable for reinforcing polymers and polymer nanocomposites. The laboratory research results indicate that only by adding 1% by weight of carbon nanotubes to the polyester resinYoung's composite modulus is increased by 35% to 43%. The study of the dynamic behavior of carbon nanotubes plays an important role in developing their application in a wide range of non-mechanical equipment such as oscillators, clocks, and nanosensors. Reliability analysis of nanoscale equipment based on carbon nanotubes requires identifying the nanotube response to the applied mechanical forces. The application of carbon nanotubes in many existing fields requires a detailed understanding of their mechanical behavior. Since nanoscale testing is very challenging and complex, theoretical modeling is particularly important for predicting carbon nanotube mechanical behavior [1-3].

As we know, various theories have been presented to investigate the dynamic displacement of beams, among which we can refer to higher-order shear deformation theories. These theories are presented to reach a more accurate answer and reduce the error caused by the previous theories. In this article, various higher-order shear deformation theories have been investigated to present their differences. The difference between these theories is in the choice of shape function, according to which they have upper limit and lower limit values.

Zhao et. al. [4] analyzed the vibrations of a purposeful functionally graded plate with porosity. The equations were derived using high-order shear deformation theory and Jacobi-Ritz theory. The effect of parameters on the vibrations of the circular plate was investigated. Xiao et al. [5] analyzed the nonlinear vibrations of nanobeam in a magnetic-electric-thermal environment. Temperature-dependent material properties are defined. The equations were

---

extracted using nonlocal and higher-order shear deformation theories, and the Galerkin method was solved. Finally, various parameters were investigated. Ramezani et al. [6] analyzed the nonlinear stability of a cylindrical shell reinforced with carbon nanotubes in a thermal environment. The von Kármán strain field is used to describe nonlinearly. The equations are derived using higher-order zigzag theory. Finally, the stress of cylindrical shells in a thermal environment is analyzed. Malabari et al. [7] presented a continuous mathematical model for analyzing the free vibrations of a CNT multilayer composite nanoplate. The relations were obtained using nonlocal strain gradient theory (NSGT). The relations were solved by the Galerkin method. Finally, various geometries on the nanoplate frequency were investigated.

Van Quyen et al. [8] analyzed the nonlinear vibrations of a carbon-nanotube-reinforced sandwich cylindrical with a honeycomb core. The sandwich panel is located in a thermal environment, and a negative Poisson's ratio is used. The Reddy higher-order theory extracted the equations, and the equations were solved using the Runge-Kutta method. Finally, various free and forced vibration parameters are investigated. Hosseini et al. [9] investigated the response of an FG nanobeam with a moving force in a thermal environment. The relations were obtained by the Hamilton principle and nonlocal theory and then solved using Laplace transform. Finally, the effect of different parameters on the response of nanobeam was investigated.

Dat et al. [10] investigated the analytical solutions for nonlinear vibration of the sandwich plate with CNT nanocomposite core in the hygro-thermal environment. Dat et al. [11] investigated the vibration analysis of FG-CNTRC plate subjected to thermo-mechanical load based on higher-order theory. Dat et al. [12] investigated the vibration of CNT plates via refined higher-order theory. Dat et al. [13] studied the geometrically nonlinear vibration analysis of sandwich nanoplates based on higher-order NSGT.

Also, in another study, Civalek [14] investigated multi-layer composite plates using the discrete singular convolution (DSC) method. Akgöz et al. [15] investigated the vibrations of the thermo-elastic micro-beam located on the elastic foundation using different theories and numerical methods. Demir et al. [16] analyzed the static analysis of nanobeam under uniform load using the finite element method. The equations are derived using the non-local Eringen theory and the Galerkin method. Finally, various parameters have been investigated.

In another study, Daikh et al. [7] investigated free vibrations, buckling, and static displacement

[17] and dynamic analysis [18] of carbon nanotubes. In another study, Eltaher et. al. [19, 20] investigated the post-buckling of carbon nanotubes on a nonlinear elastic substrate. Daikh et al. [21-23] investigated free and forced vibrations of carbon nanotubes with a moving load. Karami et al. [24-27] investigated curved structures' vibrations and dynamic and static responses reinforced with carbon nanotubes and graphene.

This paper aimed to analyze the dynamic response of carbon nanotube-reinforced composite (CNTRC) beams under a moving harmonic load. The governing equations of the CNTRC beam are obtained based on the shear deformation beam theory and Laplace transform to solve the derived differential equations. Due to this effort, an exact solution for both transverse and axial responses is obtained. Through parametric study, valuable results have been concluded related to the effect of essential parameters such as aspect ratio, different higher-order theories, harmonic frequency, and load velocity on the dynamic response of the thermoelectric CNTRC beams, and the volume fraction of CNTs in axial and transverse modes.

2. CNTRC Beams

A CNTRC beam made from a mixture of a single-walled carbon nanotube (SWCNT) and an isotropic polymer matrix is considered. The beam has a length (L), width (B), and height (H), as shown in Fig. 1.

The expressions of the effective Young and shear modulus of CNTRC beams are as follows [28, 29].
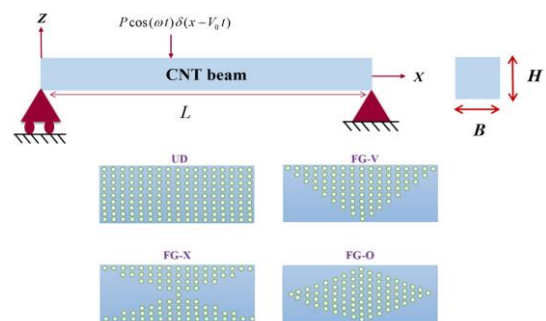

Fig. 1. Geometry of a CNTRC beam and cross-sections of four patterns of reinforcement CNTRC beam

$$E_{11} = \eta_1 V_{CN} E_{11}^{CN} + V_k E^k$$
$$\frac{\eta_2}{E_{22}} = \frac{V_{CN}}{E_{22}^{CN}} + \frac{V_k}{E^k}$$
$$\frac{\eta_3}{G_{12}} = \frac{V_{CN}}{G_{12}^{CN}} + \frac{V_k}{G^k}$$

(1)

E_{11}^{CN} and G_{12}^{CN} are defined as Young and shear modulus. E^k And G^k as the polymer matrix's

corresponding material properties. Also, V_{CN} and V_k are the volume fractions for CNT and the polymer matrix, with the relation of $V_{CN} + V_k = 1$. By using the same rule, Poisson's ratio (υ) and mass density (ρ) of the beam are written as [30]:

$$\upsilon_h = V_{CN}\upsilon_{CN} + V_k\upsilon^k \tag{2}$$

$$\rho_h = V_{CN}\rho_{CN} + V_k\rho^k \tag{3}$$

where υ_{CN}, υ^k, ρ_{CN} and ρ^k are the Poisson's ratios, densities, and thermal expansion coefficients of the carbon nanotube and polymer matrix. Different patterns of CNT reinforcement distribution are given below [31]:

UD-Beam: $V_{CN} = V_{CN}^*$

V-Beam: $V_{CN} = (1 + \dfrac{2z}{h})V_{CN}^*$

O-Beam: $V_{CN} = 2(1 - \dfrac{2|z|}{h})V_{CN}^*$ $\qquad$ (4)

X-Beam: $V_{CN} = 2(\dfrac{2|z|}{h})V_{CN}^*$

where volume fraction (V_{CN}^*) is the given volume fraction of carbon nanotubes [31]:

$$V_{CN}^* = \frac{W_{CN}}{W_{CN} + (\frac{\rho_{CN}}{\rho_k}) - (\frac{\rho_{CN}}{\rho_k})W_{CN}} \tag{5}$$

where W_{CN} is the mass fraction of CNTs $\eta_1 = 1.2833, \eta_2 = \eta_3 = 1.0556, V_{CN}^* = 0.12$ [29].

3. Equations of Motion

According to shear deformation beam theory, the displacement field at any point is as follows [32]:

$$u(x,z,t) = u_0 - z\frac{\partial w_0(x,t)}{\partial x} + \Psi(z)f_0(x,t)$$
$$w(x,z,t) = w_0(x,t) \tag{6}$$

where u_0 and w_0 are the axial and transverse displacement at the reference plane of the beam, $\Psi(z)$ is the shape function. f_0 and $\Psi(z)$, defined as [33]:

$$f_0(x,t) = \frac{\partial w_0(x,t)}{\partial x} - \phi_0(x,t)$$
$$\Psi(z) = \tan(\frac{\pi z}{2h})m^{\sec(\frac{\pi z}{2h})} \tag{7}$$

For other shear strain shape functions, see Table 1 [33].

Table 1. Shear strain shape function $\Psi(z)$ values.

Theories	Shape functions
Hyperbolic shear deformation theory	$\Psi(z) = h\sinh(\frac{z}{h}) - z\cosh(\frac{1}{2})$
Bonilla	$\Psi(z) = \tan(\frac{\pi z}{2h})m^{\sec(\frac{\pi z}{2h})}$
Reddy	$\Psi(z) = z^3$
Karama	$\Psi(z) = ze^{-2(\frac{z}{h})^2}$
Mantari	$\Psi(z) = \sin(\frac{\pi z}{h})e^{m\cos(\frac{\pi z}{h})}$

where ϕ_0 is the bending rotation of the reference plane, $m = 0.03$ and t is time. The expression of shear and normal strain components in Eq. (6).

$$\varepsilon_{xx} = \frac{\partial u_0}{\partial x} - z\frac{\partial^2 w_0}{\partial x^2} + \Psi(z)(\frac{\partial^2 w_0}{\partial x^2} - \frac{\partial \phi_0}{\partial x}) \tag{8}$$

$$\gamma_{xz} = \frac{\partial \Psi(z)}{\partial z}(\frac{\partial w_0}{\partial x} - \phi_0) \tag{9}$$

The normal and shear stress, respectively σ_{xx} and σ_{xz} as:

$$\sigma_{xx} = E_{11}(z,t)\varepsilon_{xx,x} \tag{10}$$

$$\sigma_{xz} = Q_{55}(z)\gamma_{xz}, \qquad Q_{55}(z) = G_{12}(z) \tag{11}$$

Using the Hamilton principle as follows [34]:

$$\int_{t_1}^{t_2}(\delta V - \delta K + \delta U)dt = 0, \tag{12}$$

where δK is the virtual kinetic energy, and δU is the virtual of the total strain energy, δV is the virtual work done by external loads. The initial and final time is defined as t_1 and t_2.

$$\delta U = \iint_A \int_0^L (\sigma_{xx}\delta\varepsilon_{xx} + \sigma_{xz}\delta\gamma_{xz})dxdA =$$
$$\int_0^L (N_x\frac{d\delta u_0}{dx} - M_x\frac{d^2\delta w_0}{dx^2} + \tag{13}$$
$$P_x(\frac{d^2\delta w_0}{dx^2} - \frac{d\delta\phi_0}{dx}) + Q_x(\frac{d\delta w_0}{dx} - \delta\phi_0))dA$$

The virtual work done (δV) can be expressed as:

$$\delta V = -\int_0^L (q\delta w_0)dx$$
$$q = P\cos(\omega t)\delta(x - V_0 t) \tag{14}$$

where the transverse load *(q)*, $\cos(\omega t)$ is concentrated moving the harmonic load, ω is excitation frequency, and $\delta(.)$ is Dirac delta function.

For the dynamic model, (δK) is required for the equations of motion:

$$\delta K = \int_0^L \rho(z)[\dot{u}\delta\dot{u} + \dot{w}\delta\dot{w}]dAdx =$$

$$\int_0^L \begin{Bmatrix} I_0(\dot{u}_0\delta\dot{u}_0 + \dot{w}_0\delta\dot{w}_0) - I_1(\frac{d\dot{w}_0}{dx}\delta\dot{u}_0 + \\ \dot{u}_0\frac{d\delta\dot{w}_0}{dx}) + I_2(\frac{d\dot{w}_0}{dx}\frac{d\delta\dot{w}_0}{dx}) + \\ I_3(\frac{d\dot{w}_0}{dx}\delta\dot{u}_0 - \dot{\phi}_0\delta\dot{u}_0 + \dot{u}_0\frac{d\delta\dot{w}_0}{dx} - \\ \dot{u}_0\delta\dot{\phi}_0) + I_4(\dot{\phi}_0\frac{d\delta\dot{w}_0}{dx} - 2\frac{d\dot{w}_0}{dx}\frac{d\delta\dot{w}_0}{dx} + \\ \frac{d\dot{w}_0}{dx}\delta\dot{\phi}_0) + I_5(\frac{d\dot{w}_0}{dx}\frac{d\delta\dot{w}_0}{dx} - \\ \dot{\phi}_0\frac{d\delta\dot{w}_0}{dx} - \frac{d\dot{w}_0}{dx}\delta\dot{\phi}_0 + \dot{\phi}_0\delta\dot{\phi}_0) \end{Bmatrix}dx \quad (15)$$

The stress results are extracted as:

$$N_x = \int_A \sigma_{xx}dA \quad (16)$$

$$M_x = \int_A z\sigma_{xx}dA \quad (17)$$

$$P_x = \int_A \Psi(z)\sigma_{xx}dA \quad (18)$$

$$Q_x = \int_A \frac{d\Psi(z)}{dz}\sigma_{xz}dA \quad (19)$$

N_x, M_x, P_x, and Q_x are the stress resultants in the normal bending moment, higher-order generalized, and shear force. I_i $(i = 0, 1, 2...5)$ are the mass moments of inertia:

$$[I_0, I_1, I_2] = \int_A \rho(z)[1, z, z^2]dA \quad (20)$$

$$[I_3, I_4] = \int_A \rho(z)\Psi(z)[1, z]dA \quad (21)$$

$$I_5 = \int_A \rho(z)\Psi^2(z)dA \quad (22)$$

Using Eq. (12) and, Eqs. (13)-(15) with solving the relationship and factorization, the equilibrium equation results in the following effect:

$$\delta u_0 : \frac{dN_x}{dx} = I_0\ddot{u}_0 - I_1\frac{d\ddot{w}_0}{dx} + I_3(\frac{d\ddot{w}_0}{dx} - \ddot{\phi}_0)$$

$$\delta w_0 : \frac{d^2P_x}{dx^2} - \frac{d^2M_x}{dx^2} + \frac{dQ_x}{dx} - q =$$

$$I_0\ddot{w}_0 - I_1\frac{d\ddot{u}_0}{dx} + I_2\frac{d^2\ddot{w}_0}{dx^2} + I_3\frac{d\ddot{u}_0}{dx} +$$

$$I_4(\frac{d\ddot{\phi}_0}{dx} - 2\frac{d^2\ddot{w}_0}{dx^2}) + I_5(\frac{d^2\ddot{w}_0}{dx^2} - \frac{d\ddot{\phi}_0}{dx}) \quad (23)$$

$$\delta\phi_0 : -\frac{dP_x}{dx} - Q_x = -I_3\ddot{u}_0 +$$

$$I_4\frac{d\ddot{w}_0}{dx} - I_5(\frac{d\ddot{w}_0}{dx} - \ddot{\phi}_0)$$

From the above equations:

$$N_x = A_{11}\frac{du_0}{dx} - B_{11}\frac{d^2w_0}{dx^2} + C_{11}(\frac{d^2w_0}{dx^2} - \frac{d\phi_0}{dx}) \quad (24)$$

$$M_x = B_{11}\frac{du_0}{dx} - D_{11}\frac{d^2w_0}{dx^2} + E_{11}(\frac{d^2w_0}{dx^2} - \frac{d\phi_0}{dx}) \quad (25)$$

$$P_x = C_{11}\frac{du_0}{dx} - E_{11}\frac{d^2w_0}{dx^2} + H_{11}(\frac{d^2w_0}{dx^2} - \frac{d\phi_0}{dx}) \quad (26)$$

$$Q_x = A_{55}(\frac{dw_0}{dx} - \phi_0) \quad (27)$$

where:

$$[A_{11}, B_{11}, D_{11}] = \int_A Q_{11}[1, z, z^2]dA \quad (28)$$

$$[C_{11}, E_{11}] = \int_A Q_{11}\Psi(z)[1, z]dA \quad (29)$$

$$H_{11} = \int_A Q_{11}\Psi^2(z)dA \quad (30)$$

$$A_{55} = \int_A Q_{55}(\frac{d\Psi(z)}{dz})^2 dA \quad (31)$$

The stress resultants of Eqs. (24)-(27) are substituted into Eq. (23) to obtain the relations of motion:

$$A_{11}\frac{d^2u_0}{dx^2} - B_{11}\frac{d^3w_0}{dx^3} + C_{11}(\frac{d^3w_0}{dx^3} - \frac{d^2\phi_0}{dx^2}) =$$

$$I_0\ddot{u}_0 - I_1\frac{d\ddot{w}_0}{dx} + I_3(\frac{d\ddot{w}_0}{dx} - \ddot{\phi}_0) \quad (32)$$

$$C_{11}\frac{d^3u_0}{dx^3} - E_{11}\frac{d^4w_0}{dx^4} + H_{11}(\frac{d^4w_0}{dx^4} - \frac{d^3\phi_0}{dx^3}) -$$

$$B_{11}\frac{d^3u_0}{dx^3} + D_{11}\frac{d^4w_0}{dx^4} - E_{11}(\frac{d^4w_0}{dx^4} - \frac{d^3\phi_0}{dx^3}) +$$

$$A_{55}(\frac{d^2w_0}{dx^2} - \frac{d\phi_0}{dx}) - q = I_0\ddot{w}_0 - I_1\frac{d\ddot{u}_0}{dx} +$$

$$I_2\frac{d^2\ddot{w}_0}{dx^2} + I_3\frac{d\ddot{u}_0}{dx} + I_4(\frac{d\ddot{\phi}_0}{dx} - 2\frac{d^2\ddot{w}_0}{dx^2}) +$$

$$I_5(\frac{d^2\ddot{w}_0}{dx^2} - \frac{d\ddot{\phi}_0}{dx}) \quad (33)$$

$$-C_{11}\frac{d^2u_0}{dx^2} + E_{11}\frac{d^3w_0}{dx^3} - H_{11}(\frac{d^3w_0}{dx^3} - \frac{d^2\phi_0}{dx^2}) -$$

$$A_{55}(\frac{dw_0}{dx} - \phi_0) = -I_3\ddot{u}_0 + I_4\frac{d\ddot{w}_0}{dx} - I_5(\frac{d\ddot{w}_0}{dx} - \ddot{\phi}_0) \quad (34)$$

Assuming [35]:

$$u_0(x,t) = \sum_{n=1}^{\infty} U_n(t)\cos(\frac{n\pi x}{L}) \quad (35)$$

$$\phi_0(x,t) = \sum_{n=1}^{\infty} \Phi_n(t)\cos(\frac{n\pi x}{L}) \quad (36)$$

$$w_0(x,t) = \sum_{n=1}^{\infty} W_n(t)\sin(\frac{n\pi x}{L}) \quad (37)$$

$U_n(t)$, $W_n(t)$ and $\Phi_n(t)$ are the unknown Fourier coefficients to be determined for each n value. By using the general property of the Dirac Delta function [35]:

$$\delta(x - V_0t) = 2\sum_{n=1}^{\infty} \sin(\frac{n\pi x}{L})\sin(\frac{n\pi V_0t}{L}) \quad (38)$$

Assuming: $\quad \alpha = (\frac{n\pi}{L})$

According to the exact solution provided to investigate the forced vibrations and the difficulty of solving a couple of equations for the moving load state, it should be noted that the provided method can only be solved for simply supported boundary conditions and other boundary conditions, solving the inverse Laplace equations, It is not possible. For initial conditions, Simply-support:

$$W_n(0) = \dot{W}_n(0) = U_n(0) = \dot{U}_n(0) =$$
$$\Phi_n(0) = \dot{\Phi}_n(0) = 0 \tag{39}$$

To solve the system of the differential Eqs. (32)-(34) in the time domain. By recalling this transform:

$$L\left[\ddot{W}_n(t)\right] = s^2 W_n(s) - s W_n(0) - \dot{W}_n(0),$$
$$W_n(s) = L[W_n(t)]$$
$$L\left[\ddot{U}_n(t)\right] = s^2 U_n(s) - s U_n(0) - \dot{U}_n(0),$$
$$U_n(s) = L[U_n(t)] \tag{40}$$
$$L\left[\ddot{\Phi}_n(t)\right] = s^2 \Phi_n(s) - s \Phi_n(0) - \dot{\Phi}_n(0),$$
$$\Phi_n(s) = L[\Phi_n(t)]$$

where applying Laplace Transform in Eqs. (32)-(34), the system of equation is obtained as follow:

$$\begin{pmatrix} K_{11} & K_{12} & K_{13} \\ K_{21} & K_{22} & K_{23} \\ K_{31} & K_{32} & K_{33} \end{pmatrix} \begin{Bmatrix} U_n(s) \\ W_n(s) \\ \Phi_n(s) \end{Bmatrix} = \begin{Bmatrix} 0 \\ F \\ 0 \end{Bmatrix} \tag{41}$$

where:

$$K_{11} = A_{11}\alpha^2 + I_0 s^2, K_{12} = K_{21} = B_{11}\alpha^3 - C_{11}\alpha +$$
$$I_1\alpha s^2 - I_3\alpha s^2, K_{13} = K_{31} = C_{11}\alpha^2 + I_3 s^2,$$
$$K_{22} = -2E_{11}\alpha^4 + H_{11}\alpha^4 + D_{11}\alpha^4 + A_{55}\alpha^2 +$$
$$I_0 s^2 + I_2\alpha^2 s^2 - 2I_4\alpha^2 s^2 + I_5\alpha^2 s^2 \tag{42}$$
$$K_{23} = K_{32} = -H_{11}\alpha^3 + E_{11}\alpha^3 - A_{55}\alpha + I_4\alpha s^2 - I_5\alpha s^2,$$
$$K_{33} = H_{11}\alpha^2 + A_{55} + I_5 s^2$$
$$F = \frac{P(\omega + \alpha V_0)}{s^2 + (\omega + \alpha V_0)^2} + \frac{P(\omega - \alpha V_0)}{s^2 + (\omega - \alpha V_0)^2}$$

By solving the Eq. (41), $U_n(s)$, $W_n(s)$ and $\Phi_n(s)$ are obtained as:

$$\begin{pmatrix} U_n(s) \\ W_n(s) \\ \Phi_n(s) \end{pmatrix} = \frac{1}{\det(K)} \begin{pmatrix} F(-K_{13}K_{23} + K_{12}K_{33}) \\ F(K_{13}^2 - K_{11}K_{33}) \\ -F(K_{12}K_{13} - K_{11}K_{23}) \end{pmatrix} \tag{43}$$

$$\det(K) = K_{13}^2 K_{22} - 2K_{12}K_{13}K_{23} + K_{11}K_{23}^2 + K_{12}^2 K_{33} - K_{11}K_{22}K_{33}$$

By applying an inverse Laplace transform to Eq. (43), the responses of the thermoelectric CNTRC beam are obtained:

$$U_n(x,t) = \frac{1}{y_2}\left(\frac{y_1 \sin\left[\sqrt{a_{25}}\,t\right]}{\sqrt{a_{25}}}\right) + \frac{1}{y_4}\left(\frac{y_3 \sin\left[\sqrt{a_{27}}\,t\right]}{\sqrt{a_{27}}}\right) +$$
$$\frac{\begin{pmatrix} -g_6\left(f_0 + x_1(f_2 + f_4 x_1)\right)\sqrt{x_2}\,(x_2 - x_3)\sqrt{x_3}\,\sinh\left[t\sqrt{x_1}\right] + \\ g_6\sqrt{x_1}\left((f_0 + x_2(f_2 + f_4 x_2))(x_1 - x_3)\sqrt{x_3}\,\sinh\left[t\sqrt{x_2}\right] + \\ \sqrt{x_2}\,(-x_1 + x_2)\left(f_0 + x_3(f_2 + f_4 x_3)\right)\sinh\left[t\sqrt{x_3}\right]\right) \end{pmatrix}}{\sqrt{x_1}\sqrt{x_2}\sqrt{x_3}\left(g_2 g_4 - 3g_0 g_6 + 2g_6^2\left(x_1 x_2^2 + x_1^2 x_3 + x_2 x_3^2\right)\right)} \tag{44}$$

$$W_n(x,t) = \frac{1}{y_2}\left(\frac{y_5 \sin\left[\sqrt{a_{25}}\,t\right]}{\sqrt{a_{25}}}\right) + \frac{1}{y_4}\left(\frac{y_6 \sin\left[\sqrt{a_{27}}\,t\right]}{\sqrt{a_{27}}}\right) +$$
$$\frac{\begin{pmatrix} -g_6\left(J_0 + x_1(J_2 + J_4 x_1)\right)\sqrt{x_2}\,(x_2 - x_3)\sqrt{x_3}\,\sinh\left[t\sqrt{x_1}\right] + \\ g_6\sqrt{x_1}\left((J_0 + x_2(J_2 + J_4 x_2))(x_1 - x_3)\sqrt{x_3}\,\sinh\left[t\sqrt{x_2}\right] + \\ \sqrt{x_2}\,(-x_1 + x_2)\left(J_0 + x_3(J_2 + J_4 x_3)\right)\sinh\left[t\sqrt{x_3}\right]\right) \end{pmatrix}}{\sqrt{x_1}\sqrt{x_2}\sqrt{x_3}\left(g_2 g_4 - 3g_0 g_6 + 2g_6^2\left(x_1 x_2^2 + x_1^2 x_3 + x_2 x_3^2\right)\right)} \tag{45}$$

$$\Phi_n(x,t) = \frac{1}{y_2}\left(\frac{y_7 \sin\left[\sqrt{a_{25}}\,t\right]}{\sqrt{a_{25}}}\right) + \frac{1}{y_4}\left(\frac{y_8 \sin\left[\sqrt{a_{27}}\,t\right]}{\sqrt{a_{27}}}\right) +$$
$$\frac{\begin{pmatrix} -g_6\left(R_0 + x_1(R_2 + R_4 x_1)\right)\sqrt{x_2}\,(x_2 - x_3)\sqrt{x_3}\,\sinh\left[t\sqrt{x_1}\right] + \\ g_6\sqrt{x_1}\left((R_0 + x_2(R_2 + R_4 x_2))(x_1 - x_3)\sqrt{x_3}\,\sinh\left[t\sqrt{x_2}\right] + \\ \sqrt{x_2}\,(-x_1 + x_2)\left(R_0 + x_3(R_2 + R_4 x_3)\right)\sinh\left[t\sqrt{x_3}\right]\right) \end{pmatrix}}{\sqrt{x_1}\sqrt{x_2}\sqrt{x_3}\left(g_2 g_4 - 3g_0 g_6 + 2g_6^2\left(x_1 x_2^2 + x_1^2 x_3 + x_2 x_3^2\right)\right)} \tag{46}$$

4. Results and Discussions

The results presented in this chapter are related to analyzing the axial and transverse dynamic response of CNTRC beams under moving harmonic force. Also, the influence of parameters such as aspect ratio, different higher-order theories, excitation frequency, the volume fraction of carbon nanotubes, and load velocity on the response of the thermoelectric CNTRC beams in axial and transverse modes were investigated.

The relations described in Eq. (47) are performed to calculate dimensionless natural frequencies.

$$\bar{\omega} = \lambda \frac{L^2}{h}\sqrt{\frac{\rho^k}{E^k}} \tag{47}$$

Frequency values were compared, and good validity in terms of frequency values was observed. The results are compared with Wattanasakulpong et. al. [32], given in Table 2. Also, the dimensions of the beam are: $\frac{L}{h} = 100$, $L = 100$.

The effective material properties are given as follows. $\upsilon^k = 0.3$; $\rho^k = 1190\frac{\text{Kg}}{\text{m}^3}$ and $E^k = 2.5\,\text{GPa}$. For reinforcement material: $\upsilon_{CN} = 0.19$; $\rho_{CN} = 1400\frac{\text{Kg}}{\text{m}^3}$; $E_{11}^{CN} = 600\,\text{GPa}$; $E_{22}^{CN} = 10\,\text{GPa}$ and $G_{12}^{CN} = 17.2\,\text{GPa}$ [29].

As shown in Table 2, among different types of CNTRC beams, frequency O-Beam is the lowest, and X-Beam is the highest.

Figures 2-4 show the axial displacement in terms of time. Figure 2 shows the axial displacements for different harmonic frequencies for V-Beam. As can be seen, the moving harmonic force decreases, and the axial displacement also decreases with increasing harmonic frequency.

Table 2. Comparisons of fundamental frequencies $\frac{L}{h} = 15, V_{CN}^* = 0.12$

	UD-Beab	V-Beab	O-Beab	X-Beab
$\bar{\omega}_1$	0.974908	0.745672	1.11562	0.844435
$\bar{\omega}_1$ [32]	0.9745	0.7454	1.1151	0.8441
$\bar{\omega}_2$	2.88138	2.39797	3.10205	2.6492
$\bar{\omega}_3$	4.93056	4.29371	5.16984	4.68817
$\bar{\omega}_4$	7.01828	6.22862	7.2849	6.79126
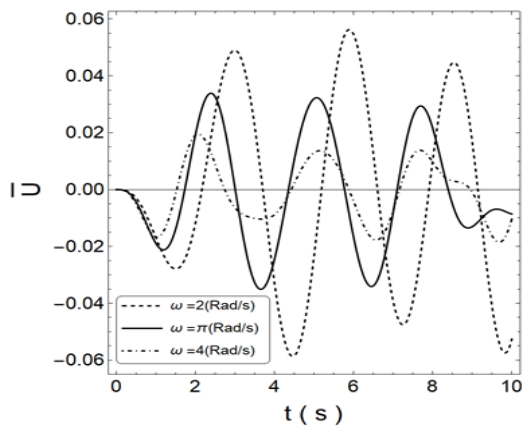
Fig. 2. Variation of dimensionless deflection V-Beam versus time for three different excitation frequencies

$$V_0 = 10(\frac{m}{s}), \frac{L}{h} = 100$$

Fig. 4. Variation of dimensionless deflection V-Beam versus time for five velocities $\frac{L}{h} = 100, \omega = 1.115(\frac{Rad}{s})$

Figure 3 shows the axial displacement for different aspect ratios for V-Beam. The axial displacement increases with the increasing aspect ratio.
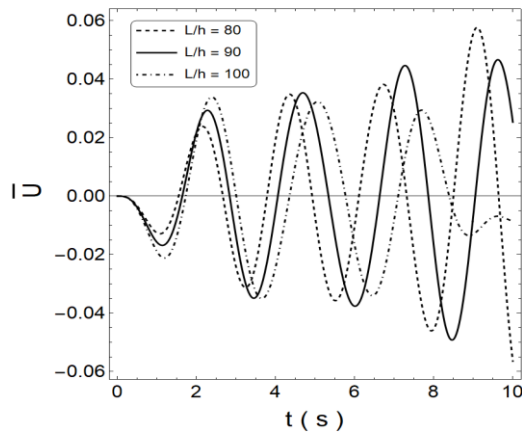
It should be noted that the axial displacement diagram has values for the states where the arrow is close to state FG and zero for other states, for example, UD-Beam.

Fig. 3. Variation of dimensionless deflection V-Beam versus time for three aspect ratios $V_0 = 10(\frac{m}{s}), \omega = \pi(\frac{Rad}{s})$

Fig. 5. Variation of dimensionless deflection X-Beam versus time for five different velocities of moving load

$$\frac{L}{h} = 100, \omega = \pi(\frac{Rad}{s})$$

Figure 4 shows the axial displacements for different velocities for V-Beam. As can be seen, the graph increases with the speed of the extreme points.
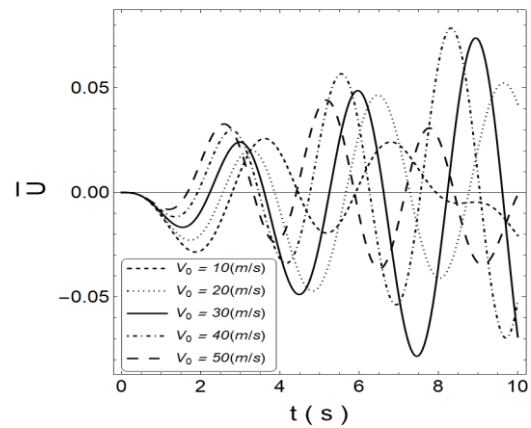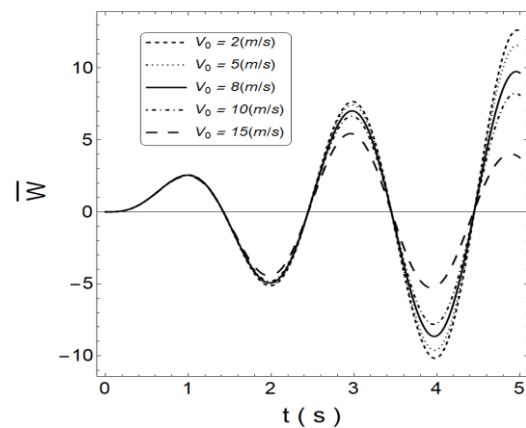
Similarly, the variation of transverse dynamic deflection versus time for X-Beam for different velocities and aspect ratio of moving harmonic load is illustrated in Figs. 5-6.

The results of these figures show that as the speed increases, the peak point of the plot decreases to shorter times. Also, the transverse displacement has increased with an increasing aspect ratio.
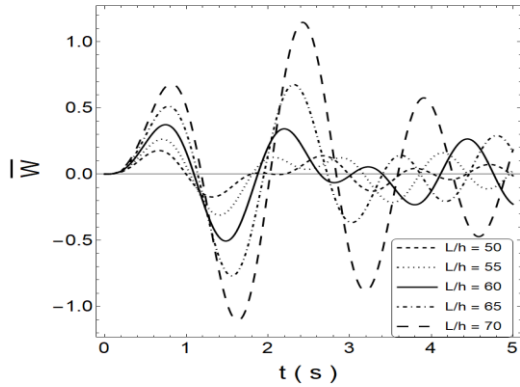

Fig. 6. Variation of dimensionless deflection X-Beam versus time for five different aspect ratios of moving load

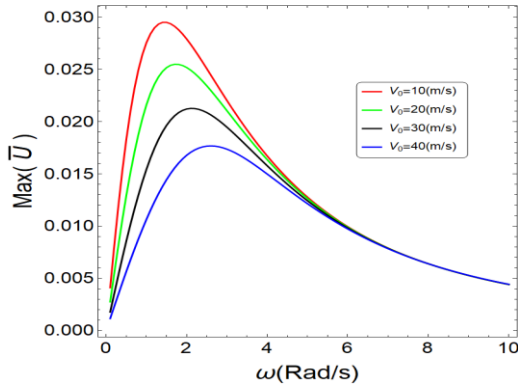$$V_0 = 10(\frac{m}{s}), \; \omega = \pi(\frac{Rad}{s})$$

Fig. 7. Maximum dimensionless displacements of V-Beam versus excitation frequency for four different velocity $\frac{L}{h} = 100$
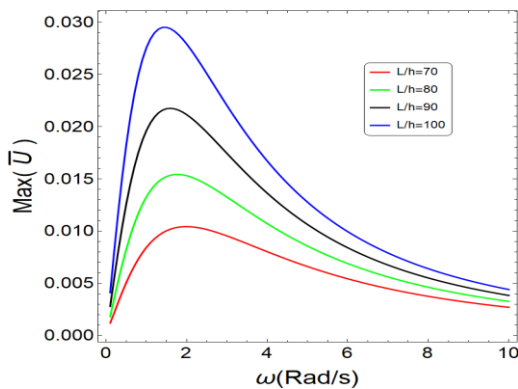

Fig. 8. Maximum dimensionless displacements of V-Beam under moving load versus excitation frequency for four different aspect ratio $V_0 = 10(\frac{m}{s})$

Figure 7 shows the maximum axial displacements of V-Beam under moving force versus excitation frequency for velocities. By increasing the speed, maximum dimensionless axial displacements decrease.

Figure 8 presents the Maximum axial displacements of V-Beam under moving force versus excitation frequency for aspect ratios. By increasing the aspect ratio, maximum dimensionless axial displacements increases.
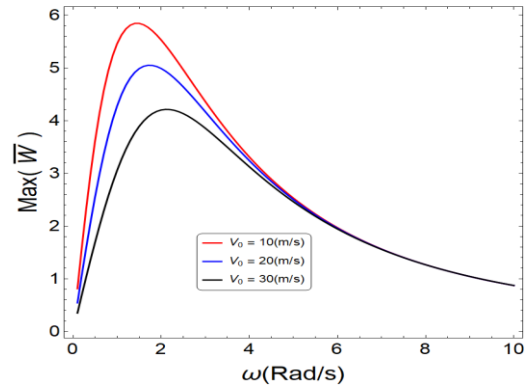

Fig. 9. Maximum dimensionless transverse displacements of V-Beam versus excitation frequency for three different velocity $\frac{L}{h} = 100$
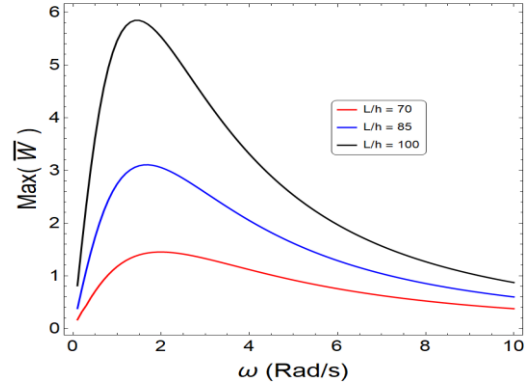

Fig. 10. Maximum dimensionless transverse displacements of V-Beam versus excitation frequency for three different aspect ratio $V_0 = 10(\frac{m}{s})$

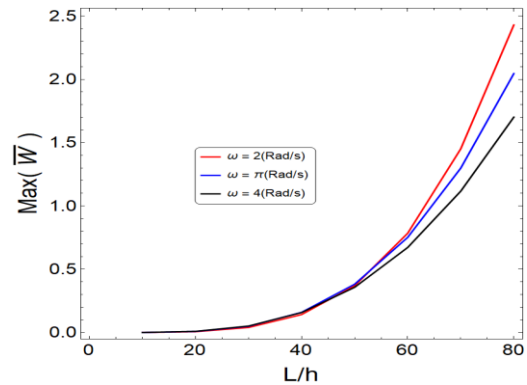**Fig. 11.** Maximum dimensionless displacements of V-Beam versus aspect ratio for three different excitation frequencies $V_0 = 10(\frac{m}{s})$

Figure 9 demonstrates maximum transverse displacements of V-Beam under moving harmonic load versus excitation frequency for velocities. By increasing the speed, maximum dimensionless transverse displacements decrease.

Fig. 10 represents the maximum transverse displacements of V-Beam under moving harmonic load versus excitation frequency for aspect ratios. By increasing the aspect ratio, maximum dimensionless transverse displacements increase.

Figure 11 illustrates the maximum transverse displacements of V-Beam under moving harmonic load versus aspect ratio for excitation frequencies. By increasing the excitation frequency, maximum dimensionless transverse displacements decrease.
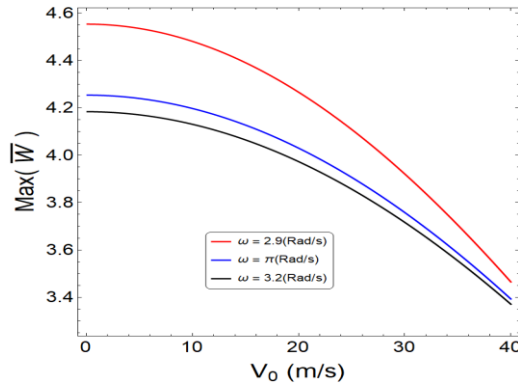

Fig. 12. Maximum dimensionless displacements of V-Beam versus velocity for three different excitation frequencies $\frac{L}{h} = 100$
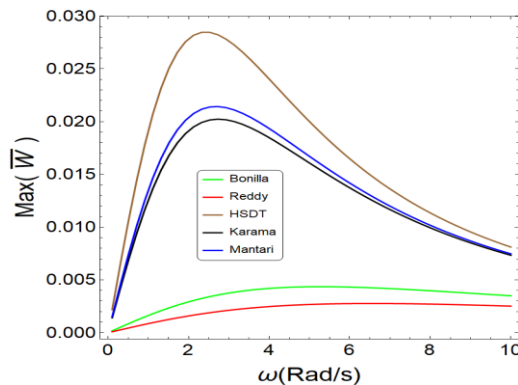

Fig. 13. Maximum dimensionless displacements of V-Beam versus excitation frequency for five different theories $V_0 = 30(\frac{m}{s}), \frac{L}{h} = 10$

Figure 12 shows the maximum transverse displacements of V-Beam under moving harmonic load versus velocity for excitation frequencies. By increasing the harmonic frequency, maximum dimensionless transverse displacements decrease.

Figure 13 presents the maximum transverse displacements of V-Beam under moving harmonic load versus excitation frequency for five theories $\frac{L}{h} = 10$. As can be seen, the theory of HSDT is a higher limit theory than the theories by Mantari, Karama, Bonilla, and Reddy, respectively.
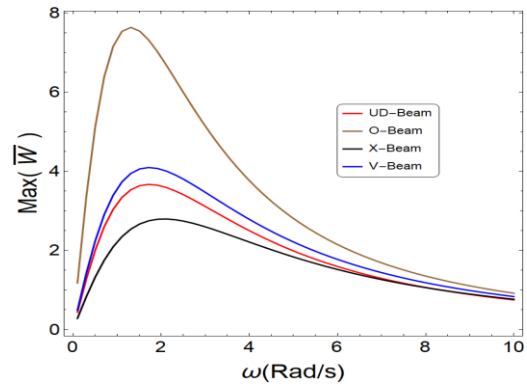

Fig. 14. Maximum dimensionless displacements of CNTRC beams versus excitation frequency $V_0 = 10(\frac{m}{s}), \frac{L}{h} = 100$

Figure 14 demonstrates the maximum transverse displacements of CNTRC beams under moving harmonic load versus excitation frequency. As seen, beams O, V, UD, and X have the highest max transverse dynamic deflection.

Table 3. Maximum transverse displacements of V-Beam for five different theories.

	$\omega = 2\,Rad\,/\,s$	$\omega = 4\,Rad\,/\,s$	$\omega = 6\,Rad\,/\,s$
Bonilla	0.0294803	0.0421119	0.0431822
Reddy	0.0160457	0.0248846	0.0276248
HSDT	0.279156	0.237664	0.162882
Karama	0.192065	0.183877	0.135907
Mantari	0.204725	0.192423	0.140346

Table 3 shows the maximum transverse displacement for three different excitation frequencies for different higher-order shear deformation theories. The difference between the theories is based on the choice of their shape function. HSDT theory has the highest displacement values. Reddy's theory has the lowest displacement values. As a result of the HSDT theory, the upper limit is also the Reddy theory, the lower limit. The type of theory chosen has an impact on the results.

5. Conclusions

This paper analyzes the dynamic response of CNTRC beams under moving harmonic force. The governing equations of the CNTRC beam are obtained based on higher-order theory, the Hamilton principle, and Laplace transforms to solve the derived differential equations.

It was found that the parameters of beam thickness, excitation frequency, and moving load speed have a significant effect on forced vibrations and transverse and axial displacement of CNTRC beams. It should be noted that the

effects created on the results are due to the changes in the stress results.

- Among CNTRC beams, the highest transverse and axial displacements are for O, V, UD, and X beams, respectively, so O-Beam has the weakest resistance to flexural loads. They increased the aspect ratio of the displacement of the CNTRC beams. Also, increasing the excitation frequency, velocity and V_{CN}^*, displacement of the CNTRC beams reduced.

- The axial displacement diagram has values for the states where the arrow is close to state FG and zero for other states, for example, UD-Beam.

- Theory HSDT is a higher limit theory than Theories by Mantari, Karama, Bonilla, and Reddy $\frac{L}{h} = 10$. Among different CNTRC beams, frequency O-Beam is the lowest, and X-Beam is the highest.

- The presented method for the boundary condition simply support.

Nomenclature

L	Length
H	Height
G	Shear modulus
E	Young's modulus
ρ	Mass density
υ	Poisson's ratio
σ_{xx}	Normal stress
σ_{xz}	Shear stress
N_x, M_x, P_x, Q_x	Stress resultants
ω	Excitation frequency
V_{CN}^*	Volume fraction
W_{CN}	Mass fraction
η_i	CNT Efficiency parameters
u_0	Axial displacement
w_0	Transverse displacement
$\Psi(z)$	Shape function
ϕ_0	Total bending rotation
t	Time
f	Transverse load
V	Velocity of moving load
U	Virtual strain energy
V	Virtual work
K	Virtual kinetic energy
I	Mass moments of inertia

Appendixes

$$u_1 = 1, \quad u_2 = \frac{-1 + I\sqrt{3}}{2}, \quad u_3 = \frac{-1 - I\sqrt{3}}{2}$$

$$\Delta_0 = g_4^2 - 3g_6 g_2, \quad \Delta_1 = 2g_4^3 - 9g_6 g_4 g_2 + 27 g_6^2 g_0,$$

$$Ci = \sqrt[3]{\frac{\Delta_1 + \sqrt{\Delta_1^2 - 4\Delta_0^3}}{2}}$$

$$x_1 = \frac{-1}{3g_6}\left(g_4 + u_1 Ci + \frac{\Delta_0}{u_1 Ci}\right)$$

$$x_2 = \frac{-1}{3g_6}\left(g_4 + u_2 Ci + \frac{\Delta_0}{u_2 Ci}\right)$$

$$x_3 = \frac{-1}{3g_6}\left(g_4 + u_3 Ci + \frac{\Delta_0}{u_3 Ci}\right)$$

(48)

$$\begin{aligned}
y_1 = & -a_7 a_{16} a_{24} - a_7 a_{17} a_{24} - a_7 a_{18} a_{24} + a_3 a_{21} a_{24} + a_4 a_{21} a_{24} + \\
& a_3 a_{22} a_{24} + a_4 a_{22} a_{24} + a_8 a_{16} a_{24} a_{25} + a_8 a_{17} a_{24} a_{25} + a_8 a_{18} a_{24} a_{25} + \\
& a_7 a_{19} a_{24} a_{25} + a_7 a_{20} a_{24} a_{25} - a_5 a_{21} a_{24} a_{25} - a_6 a_{21} a_{24} a_{25} - \\
& a_5 a_{22} a_{24} a_{25} - a_6 a_{22} a_{24} a_{25} - a_3 a_{23} a_{24} a_{25} - a_4 a_{23} a_{24} a_{25} - \\
& a_8 a_{19} a_{24} a_{25}^2 - a_8 a_{20} a_{24} a_{25}^2 + a_5 a_{23} a_{24} a_{25}^2 + a_6 a_{23} a_{24} a_{25}^2
\end{aligned}$$

(49)

$$\begin{aligned}
y_2 = & a_7^2 a_9 + a_7^2 a_{10} + a_7^2 a_{11} + a_7^2 a_{12} - 2a_3 a_7 a_{16} - 2a_4 a_7 a_{16} + \\
& a_1 a_{16}^2 - 2a_3 a_7 a_{17} - 2a_4 a_7 a_{17} + 2a_1 a_{16} a_{17} + a_1 a_{17}^2 - \\
& 2a_3 a_7 a_{18} - 2a_4 a_7 a_{18} + 2a_1 a_{16} a_{18} + 2a_1 a_{17} a_{18} + a_1 a_{18}^2 + \\
& a_3^2 a_{21} + 2a_3 a_4 a_{21} + a_4^2 a_{21} - a_1 a_9 a_{21} - a_1 a_{10} a_{21} - a_1 a_{11} a_{21} - \\
& a_1 a_{12} a_{21} + a_3^2 a_{22} + 2a_3 a_4 a_{22} + a_4^2 a_{22} - a_1 a_9 a_{22} - a_1 a_{10} a_{22} - \\
& a_1 a_{11} a_{22} - a_1 a_{12} a_{22} - a_2 a_7^2 a_{25} - 2a_7 a_8 a_9 a_{25} - 2a_7 a_8 a_{10} a_{25} - \\
& 2a_7 a_8 a_{11} a_{25} - 2a_7 a_8 a_{12} a_{25} - a_7^2 a_{13} a_{25} - a_7^2 a_{14} a_{25} - a_7^2 a_{15} a_{25} + \\
& 2a_5 a_7 a_{16} a_{25} + 2a_6 a_7 a_{16} a_{25} + 2a_3 a_8 a_{16} a_{25} + 2a_4 a_8 a_{16} a_{25} - \\
& a_2 a_{16}^2 a_{25} + 2a_5 a_7 a_{17} a_{25} + 2a_6 a_7 a_{17} a_{25} + 2a_3 a_8 a_{17} a_{25} + \\
& 2a_4 a_8 a_{17} a_{25} - 2a_2 a_{16} a_{17} a_{25} - a_2 a_{17}^2 a_{25} + 2a_5 a_7 a_{18} a_{25} + \\
& 2a_6 a_7 a_{18} a_{25} + 2a_3 a_8 a_{18} a_{25} + 2a_4 a_8 a_{18} a_{25} - 2a_2 a_{16} a_{18} a_{25} - \\
& 2a_2 a_{17} a_{18} a_{25} - a_2 a_{18}^2 a_{25} + 2a_3 a_7 a_{19} a_{25} + 2a_4 a_7 a_{19} a_{25} - \\
& 2a_1 a_{16} a_{19} a_{25} - 2a_1 a_{17} a_{19} a_{25} - 2a_1 a_{18} a_{19} a_{25} + 2a_3 a_7 a_{20} a_{25} + \\
& 2a_4 a_7 a_{20} a_{25} - 2a_1 a_{16} a_{20} a_{25} - 2a_1 a_{17} a_{20} a_{25} - 2a_1 a_{18} a_{20} a_{25} + \\
& a_1 a_2 a_{21} a_{25} - 2a_3 a_5 a_{21} a_{25} - 2a_4 a_5 a_{21} a_{25} - 2a_3 a_6 a_{21} a_{25} - \\
& 2a_4 a_6 a_{21} a_{25} + a_2 a_9 a_{21} a_{25} + a_2 a_{10} a_{21} a_{25} + a_2 a_{11} a_{21} a_{25} + \\
& a_2 a_{12} a_{21} a_{25} + a_1 a_{13} a_{21} a_{25} + a_1 a_{14} a_{21} a_{25} + a_1 a_{15} a_{21} a_{25} + \\
& a_1 a_2 a_{22} a_{25} - 2a_3 a_5 a_{22} a_{25} - 2a_4 a_5 a_{22} a_{25} - 2a_3 a_6 a_{22} a_{25} - \\
& 2a_4 a_6 a_{22} a_{25} + a_2 a_9 a_{22} a_{25} + a_2 a_{10} a_{22} a_{25} + a_2 a_{11} a_{22} a_{25} + \\
& a_2 a_{12} a_{22} a_{25} + a_1 a_{13} a_{22} a_{25} + a_1 a_{14} a_{22} a_{25} + a_1 a_{15} a_{22} a_{25} - \\
& a_3^2 a_{23} a_{25} - 2a_3 a_4 a_{23} a_{25} - a_4^2 a_{23} a_{25} + a_1 a_9 a_{23} a_{25} + a_1 a_{10} a_{23} a_{25} + \\
& a_1 a_{11} a_{23} a_{25} + a_1 a_{12} a_{23} a_{25} + 2a_2 a_7 a_8 a_{25}^2 + a_8^2 a_9 a_{25}^2 + a_8^2 a_{10} a_{25}^2 + \\
& a_8^2 a_{11} a_{25}^2 + a_8^2 a_{12} a_{25}^2 + 2a_7 a_8 a_{13} a_{25}^2 + 2a_7 a_8 a_{14} a_{25}^2 + \\
& 2a_7 a_8 a_{15} a_{25}^2 - 2a_5 a_8 a_{16} a_{25}^2 - 2a_6 a_8 a_{16} a_{25}^2 - 2a_5 a_8 a_{17} a_{25}^2 - \\
& 2a_6 a_8 a_{17} a_{25}^2 - 2a_5 a_8 a_{18} a_{25}^2 - 2a_6 a_8 a_{18} a_{25}^2 - 2a_5 a_7 a_{19} a_{25}^2 - \\
& 2a_6 a_7 a_{19} a_{25}^2 - 2a_3 a_8 a_{19} a_{25}^2 - 2a_4 a_8 a_{19} a_{25}^2 + 2a_2 a_{16} a_{19} a_{25}^2 + \\
& 2a_2 a_{17} a_{19} a_{25}^2 + 2a_2 a_{18} a_{19} a_{25}^2 + a_1 a_{19}^2 a_{25}^2 - 2a_5 a_7 a_{20} a_{25}^2 - \\
& 2a_6 a_7 a_{20} a_{25}^2 - 2a_3 a_8 a_{20} a_{25}^2 - 2a_4 a_8 a_{20} a_{25}^2 + 2a_2 a_{16} a_{20} a_{25}^2 + \\
& 2a_2 a_{17} a_{20} a_{25}^2 + 2a_2 a_{18} a_{20} a_{25}^2 + 2a_1 a_{19} a_{20} a_{25}^2 + a_1 a_{20}^2 a_{25}^2 - \\
& a_5^2 a_{21} a_{25}^2 + a_5^2 a_{21} a_{25}^2 + 2a_5 a_6 a_{21} a_{25}^2 + a_6^2 a_{21} a_{25}^2 - a_2 a_{13} a_{21} a_{25}^2 - \\
& a_2 a_{14} a_{21} a_{25}^2 - a_2 a_{15} a_{21} a_{25}^2 - a_5^2 a_{22} a_{25}^2 + a_5^2 a_{22} a_{25}^2 + 2a_5 a_6 a_{22} a_{25}^2 + \\
& a_6^2 a_{22} a_{25}^2 - a_2 a_{13} a_{22} a_{25}^2 - a_2 a_{14} a_{22} a_{25}^2 - a_2 a_{15} a_{22} a_{25}^2 - \\
& a_1 a_2 a_{23} a_{25}^2 + 2a_3 a_5 a_{23} a_{25}^2 + 2a_4 a_5 a_{23} a_{25}^2 + 2a_3 a_6 a_{23} a_{25}^2 + \\
& 2a_4 a_6 a_{23} a_{25}^2 - a_2 a_9 a_{23} a_{25}^2 - a_2 a_{10} a_{23} a_{25}^2 - a_2 a_{11} a_{23} a_{25}^2 - \\
& a_2 a_{12} a_{23} a_{25}^2 - a_1 a_{13} a_{23} a_{25}^2 - a_1 a_{14} a_{23} a_{25}^2 - a_1 a_{15} a_{23} a_{25}^2 - \\
& a_2 a_8^2 a_{25}^3 - a_8^2 a_{13} a_{25}^3 - a_8^2 a_{14} a_{25}^3 - a_8^2 a_{15} a_{25}^3 + 2a_5 a_8 a_{19} a_{25}^3 + \\
& 2a_6 a_8 a_{19} a_{25}^3 - a_2 a_{19}^2 a_{25}^3 + 2a_5 a_8 a_{20} a_{25}^3 + 2a_6 a_8 a_{20} a_{25}^3 - \\
& 2a_2 a_{19} a_{20} a_{25}^3 - a_2 a_{20}^2 a_{25}^3 + a_5^2 a_{23} a_{25}^3 - a_5^2 a_{23} a_{25}^3 - 2a_5 a_6 a_{23} a_{25}^3 - \\
& a_6^2 a_{23} a_{25}^3 + a_2 a_{13} a_{23} a_{25}^3 + a_2 a_{14} a_{23} a_{25}^3 + a_2 a_{15} a_{23} a_{25}^3
\end{aligned}$$

(50)

$$y_3 = -a_7 a_{16} a_{26} - a_7 a_{17} a_{26} - a_7 a_{18} a_{26} + a_3 a_{21} a_{26} + a_4 a_{21} a_{26} +$$
$$a_3 a_{22} a_{26} + a_4 a_{22} a_{26} + a_8 a_{16} a_{26} a_{27} + a_8 a_{17} a_{26} a_{27} +$$
$$a_8 a_{18} a_{26} a_{27} + a_7 a_{19} a_{26} a_{27} + a_7 a_{20} a_{26} a_{27} - a_5 a_{21} a_{26} a_{27} -$$
$$a_6 a_{21} a_{26} a_{27} - a_5 a_{22} a_{26} a_{27} - a_6 a_{22} a_{26} a_{27} - a_3 a_{23} a_{26} a_{27} -$$
$$a_4 a_{23} a_{26} a_{27} - a_8 a_{19} a_{26} a_{27}^2 - a_8 a_{20} a_{26} a_{27}^2 + a_5 a_{23} a_{26} a_{27}^2 +$$
$$a_6 a_{23} a_{26} a_{27}^2$$

$$y_4 = a_7^2 a_9 + a_7^2 a_{10} + a_7^2 a_{11} + a_7^2 a_{12} - 2a_3 a_7 a_{16} - 2a_4 a_7 a_{16} +$$
$$a_1 a_{16}^2 - 2a_3 a_7 a_{17} - 2a_4 a_7 a_{17} + 2a_1 a_{16} a_{17} + a_1 a_{17}^2 -$$
$$2a_3 a_7 a_{18} - 2a_4 a_7 a_{18} + 2a_1 a_{16} a_{18} + 2a_1 a_{17} a_{18} + a_1 a_{18}^2 +$$
$$a_3^2 a_{21} + 2a_3 a_4 a_{21} + a_4^2 a_{21} - a_1 a_9 a_{21} - a_1 a_{10} a_{21} - a_1 a_{11} a_{21} -$$
$$a_1 a_{12} a_{21} + a_3^2 a_{22} + 2a_3 a_4 a_{22} + a_4^2 a_{22} - a_1 a_9 a_{22} - a_1 a_{10} a_{22} -$$
$$a_1 a_{11} a_{22} - a_1 a_{12} a_{22} - a_2 a_7^2 a_{27} - 2a_7 a_8 a_9 a_{27} - 2a_7 a_8 a_{10} a_{27} -$$
$$2a_7 a_8 a_{11} a_{27} - 2a_7 a_8 a_{12} a_{27} - a_7^2 a_{13} a_{27} - a_7^2 a_{14} a_{27} -$$
$$a_7^2 a_{15} a_{27} + 2a_5 a_7 a_{16} a_{27} + 2a_6 a_7 a_{16} a_{27} + 2a_3 a_8 a_{16} a_{27} +$$
$$2a_4 a_8 a_{16} a_{27} - a_2 a_{16}^2 a_{27} + 2a_5 a_7 a_{17} a_{27} + 2a_6 a_7 a_{17} a_{27} +$$
$$2a_3 a_8 a_{17} a_{27} + 2a_4 a_8 a_{17} a_{27} - 2a_2 a_{16} a_{17} a_{27} - a_2 a_{17}^2 a_{27} +$$
$$2a_5 a_7 a_{18} a_{27} + 2a_6 a_7 a_{18} a_{27} + 2a_3 a_8 a_{18} a_{27} + 2a_4 a_8 a_{18} a_{27} -$$
$$2a_2 a_{16} a_{18} a_{27} - 2a_2 a_{17} a_{18} a_{27} - a_2 a_{18}^2 a_{27} + 2a_3 a_7 a_{19} a_{27} +$$
$$2a_4 a_7 a_{19} a_{27} - 2a_1 a_{16} a_{19} a_{27} - 2a_1 a_{17} a_{19} a_{27} - 2a_1 a_{18} a_{19} a_{27} +$$
$$2a_3 a_7 a_{20} a_{27} + 2a_4 a_7 a_{20} a_{27} - 2a_1 a_{16} a_{20} a_{27} - 2a_1 a_{17} a_{20} a_{27} -$$
$$2a_1 a_{18} a_{20} a_{27} + a_1 a_2 a_{21} a_{27} - 2a_3 a_5 a_{21} a_{27} - 2a_4 a_5 a_{21} a_{27} -$$
$$2a_3 a_6 a_{21} a_{27} - 2a_4 a_6 a_{21} a_{27} + a_2 a_9 a_{21} a_{27} + a_2 a_{10} a_{21} a_{27} +$$
$$a_2 a_{11} a_{21} a_{27} + a_2 a_{12} a_{21} a_{27} + a_1 a_{13} a_{21} a_{27} + a_1 a_{14} a_{21} a_{27} +$$
$$a_1 a_{15} a_{21} a_{27} + a_1 a_2 a_{22} a_{27} - 2a_3 a_5 a_{22} a_{27} - 2a_4 a_5 a_{22} a_{27} -$$
$$2a_3 a_6 a_{22} a_{27} - 2a_4 a_6 a_{22} a_{27} + a_2 a_9 a_{22} a_{27} + a_2 a_{10} a_{22} a_{27} +$$
$$a_2 a_{11} a_{22} a_{27} + a_2 a_{12} a_{22} a_{27} + a_1 a_{13} a_{22} a_{27} + a_1 a_{14} a_{22} a_{27} +$$
$$a_1 a_{15} a_{22} a_{27} - a_3^2 a_{23} a_{27} - 2a_3 a_4 a_{23} a_{27} - a_4^2 a_{23} a_{27} + a_1 a_9 a_{23} a_{27} +$$
$$a_1 a_{10} a_{23} a_{27} + a_1 a_{11} a_{23} a_{27} + a_1 a_{12} a_{23} a_{27} + 2a_2 a_7 a_8 a_{27}^2 +$$
$$a_8^2 a_9 a_{27}^2 + a_8^2 a_{10} a_{27}^2 + a_8^2 a_{11} a_{27}^2 + a_8^2 a_{12} a_{27}^2 + 2a_7 a_8 a_{13} a_{27}^2 +$$
$$2a_7 a_8 a_{14} a_{27}^2 + 2a_7 a_8 a_{15} a_{27}^2 - 2a_5 a_8 a_{16} a_{27}^2 - 2a_6 a_8 a_{16} a_{27}^2 -$$
$$2a_5 a_8 a_{17} a_{27}^2 - 2a_6 a_8 a_{17} a_{27}^2 - 2a_5 a_8 a_{18} a_{27}^2 - 2a_6 a_8 a_{18} a_{27}^2 -$$
$$2a_5 a_7 a_{19} a_{27}^2 - 2a_6 a_7 a_{19} a_{27}^2 - 2a_3 a_8 a_{19} a_{27}^2 - 2a_4 a_8 a_{19} a_{27}^2 +$$
$$2a_2 a_{16} a_{19} a_{27}^2 + 2a_2 a_{17} a_{19} a_{27}^2 + 2a_2 a_{18} a_{19} a_{27}^2 + a_1 a_{19}^2 a_{27}^2 -$$
$$2a_5 a_7 a_{20} a_{27}^2 - 2a_6 a_7 a_{20} a_{27}^2 - 2a_3 a_8 a_{20} a_{27}^2 - 2a_4 a_8 a_{20} a_{27}^2 +$$
$$2a_2 a_{16} a_{20} a_{27}^2 + 2a_2 a_{17} a_{20} a_{27}^2 + 2a_2 a_{18} a_{20} a_{27}^2 + 2a_1 a_{19} a_{20} a_{27}^2 +$$
$$a_1 a_{20}^2 a_{27}^2 - a_2^2 a_{21} a_{27}^2 + a_5^2 a_{21} a_{27}^2 + 2a_5 a_6 a_{21} a_{27}^2 + a_6^2 a_{21} a_{27}^2 -$$
$$a_2 a_{13} a_{21} a_{27}^2 - a_2 a_{14} a_{21} a_{27}^2 - a_2 a_{15} a_{21} a_{27}^2 - a_2^2 a_{22} a_{27}^2 +$$
$$a_5^2 a_{22} a_{27}^2 + 2a_5 a_6 a_{22} a_{27}^2 + a_6^2 a_{22} a_{27}^2 - a_2 a_{13} a_{22} a_{27}^2 - a_2 a_{14} a_{22} a_{27}^2 -$$
$$a_2 a_{15} a_{22} a_{27}^2 - a_1 a_2 a_{23} a_{27}^2 + 2a_3 a_5 a_{23} a_{27}^2 + 2a_4 a_5 a_{23} a_{27}^2 +$$
$$2a_3 a_6 a_{23} a_{27}^2 + 2a_4 a_6 a_{23} a_{27}^2 - a_2 a_9 a_{23} a_{27}^2 - a_2 a_{10} a_{23} a_{27}^2 -$$
$$a_2 a_{11} a_{23} a_{27}^2 - a_2 a_{12} a_{23} a_{27}^2 - a_1 a_{13} a_{23} a_{27}^2 - a_1 a_{14} a_{23} a_{27}^2 -$$
$$a_1 a_{15} a_{23} a_{27}^2 - 2a_2 a_8^2 a_{27}^3 - a_8^2 a_{13} a_{27}^3 - a_8^2 a_{14} a_{27}^3 - a_8^2 a_{15} a_{27}^3 +$$
$$2a_5 a_8 a_{19} a_{27}^3 + 2a_6 a_8 a_{19} a_{27}^3 - a_2 a_{19}^2 a_{27}^3 + 2a_5 a_8 a_{20} a_{27}^3 +$$
$$2a_6 a_8 a_{20} a_{27}^3 - 2a_2 a_{19} a_{20} a_{27}^3 - a_2 a_{20}^2 a_{27}^3 +$$
$$a_2^2 a_{23} a_{27}^3 - a_5^2 a_{23} a_{27}^3 - 2a_5 a_6 a_{23} a_{27}^3 - a_6^2 a_{23} a_{27}^3 +$$
$$a_2 a_{13} a_{23} a_{27}^3 + a_2 a_{14} a_{23} a_{27}^3 + a_2 a_{15} a_{23} a_{27}^3$$

(51)

$$f_0 = \frac{-a_7 a_{16} a_{24} - a_7 a_{17} a_{24} - a_7 a_{18} a_{24} + a_3 a_{21} a_{24} + a_4 a_{21} a_{24} +}{a_3 a_{22} a_{24} + a_4 a_{22} a_{24}}{a_{25}} -$$
$$\frac{r_1 y_1}{a_{25} y_2} +$$
$$\frac{-a_7 a_{16} a_{26} - a_7 a_{17} a_{26} - a_7 a_{18} a_{26} + a_3 a_{21} a_{26} + a_4 a_{21} a_{26} +}{a_3 a_{22} a_{26} + a_4 a_{22} a_{26}}{a_{27}} - \frac{r_1 y_3}{a_{27} y_4}$$

(52)

$$r_1 = a_7^2 a_9 + a_7^2 a_{10} + a_7^2 a_{11} + a_7^2 a_{12} - 2a_3 a_7 a_{16} - 2a_4 a_7 a_{16} +$$
$$a_1 a_{16}^2 - 2a_3 a_7 a_{17} - 2a_4 a_7 a_{17} + 2a_1 a_{16} a_{17} + a_1 a_{17}^2 -$$
$$2a_3 a_7 a_{18} - 2a_4 a_7 a_{18} + 2a_1 a_{16} a_{18} + 2a_1 a_{17} a_{18} + a_1 a_{18}^2 + a_3^2 a_{21} +$$
$$2a_3 a_4 a_{21} + a_4^2 a_{21} - a_1 a_9 a_{21} - a_1 a_{10} a_{21} - a_1 a_{11} a_{21} -$$
$$a_1 a_{12} a_{21} + a_3^2 a_{22} + 2a_3 a_4 a_{22} + a_4^2 a_{22} - a_1 a_9 a_{22} -$$
$$a_1 a_{10} a_{22} - a_1 a_{11} a_{22} - a_1 a_{12} a_{22}$$

$$f_4 = -\frac{r_2 y_1}{y_2} - \frac{r_2 y_3}{y_4}$$

$$r_2 = a_2 a_8^2 + a_8^2 a_{13} + a_8^2 a_{14} + a_8^2 a_{15} - 2a_5 a_8 a_{19} - 2a_6 a_8 a_{19} +$$
$$a_2 a_{19}^2 - 2a_5 a_8 a_{20} - 2a_6 a_8 a_{20} + 2a_2 a_{19} a_{20} + a_2 a_{20}^2 -$$
$$a_2^2 a_{23} + a_5^2 a_{23} + 2a_5 a_6 a_{23} + a_6^2 a_{23} - a_2 a_{13} a_{23} - a_2 a_{14} a_{23} - a_2 a_{15} a_{23}$$

(53)

$$f_2 = \frac{-y_1}{a_{25}^2} - \frac{y_1 r_3}{a_{25}^2 y_2} - a_8 a_{19} a_{26} - a_8 a_{20} a_{26} + a_5 a_{23} a_{26} +$$
$$a_6 a_{23} a_{26} - \frac{r_4 y_3}{y_4}$$

$$r_3 = -a_7^2 a_9 - a_7^2 a_{10} - a_7^2 a_{11} - a_7^2 a_{12} + 2a_3 a_7 a_{16} +$$
$$2a_4 a_7 a_{16} - a_1 a_{16}^2 + 2a_3 a_7 a_{17} + 2a_4 a_7 a_{17} - 2a_1 a_{16} a_{17} -$$
$$a_1 a_{17}^2 + 2a_3 a_7 a_{18} + 2a_4 a_7 a_{18} - 2a_1 a_{16} a_{18} - 2a_1 a_{17} a_{18} -$$
$$a_1 a_{18}^2 - a_3^2 a_{21} - 2a_3 a_4 a_{21} - a_4^2 a_{21} + a_1 a_9 a_{21} + a_1 a_{10} a_{21} +$$
$$a_1 a_{11} a_{21} + a_1 a_{12} a_{21} - a_3^2 a_{22} - 2a_3 a_4 a_{22} - a_4^2 a_{22} +$$
$$a_1 a_9 a_{22} + a_1 a_{10} a_{22} + a_1 a_{11} a_{22} + a_1 a_{12} a_{22} + a_2 a_7^2 a_{25} +$$
$$2a_7 a_8 a_9 a_{25} + 2a_7 a_8 a_{10} a_{25} + 2a_7 a_8 a_{11} a_{25} + 2a_7 a_8 a_{12} a_{25} +$$
$$a_7^2 a_{13} a_{25} + a_7^2 a_{14} a_{25} + a_7^2 a_{15} a_{25} - 2a_5 a_7 a_{16} a_{25} -$$
$$2a_6 a_7 a_{16} a_{25} - 2a_3 a_8 a_{16} a_{25} - 2a_4 a_8 a_{16} a_{25} + a_2 a_{16}^2 a_{25} -$$
$$2a_5 a_7 a_{17} a_{25} - 2a_6 a_7 a_{17} a_{25} - 2a_3 a_8 a_{17} a_{25} - 2a_4 a_8 a_{17} a_{25} +$$
$$2a_2 a_{16} a_{17} a_{25} + a_2 a_{17}^2 a_{25} - 2a_5 a_7 a_{18} a_{25} - 2a_6 a_7 a_{18} a_{25} -$$
$$2a_3 a_8 a_{18} a_{25} - 2a_4 a_8 a_{18} a_{25} + 2a_2 a_{16} a_{18} a_{25} + 2a_2 a_{17} a_{18} a_{25} +$$
$$a_2 a_{18}^2 a_{25} - 2a_3 a_7 a_{19} a_{25} - 2a_4 a_7 a_{19} a_{25} + 2a_1 a_{16} a_{19} a_{25} +$$
$$2a_1 a_{17} a_{19} a_{25} + 2a_1 a_{18} a_{19} a_{25} - 2a_3 a_7 a_{20} a_{25} - 2a_4 a_7 a_{20} a_{25} +$$
$$2a_1 a_{16} a_{20} a_{25} + 2a_1 a_{17} a_{20} a_{25} + 2a_1 a_{18} a_{20} a_{25} - a_1 a_2 a_{21} a_{25} +$$
$$2a_3 a_5 a_{21} a_{25} + 2a_4 a_5 a_{21} a_{25} + 2a_3 a_6 a_{21} a_{25} + 2a_4 a_6 a_{21} a_{25} -$$
$$a_2 a_9 a_{21} a_{25} - a_2 a_{10} a_{21} a_{25} - a_2 a_{11} a_{21} a_{25} - a_2 a_{12} a_{21} a_{25} -$$
$$a_1 a_{13} a_{21} a_{25} - a_1 a_{14} a_{21} a_{25} - a_1 a_{15} a_{21} a_{25} - a_1 a_2 a_{22} a_{25} +$$
$$2a_3 a_5 a_{22} a_{25} + 2a_4 a_5 a_{22} a_{25} + 2a_3 a_6 a_{22} a_{25} + 2a_4 a_6 a_{22} a_{25} -$$
$$a_2 a_9 a_{22} a_{25} - a_2 a_{10} a_{22} a_{25} - a_2 a_{11} a_{22} a_{25} - a_2 a_{12} a_{22} a_{25} -$$
$$a_1 a_{13} a_{22} a_{25} - a_1 a_{14} a_{22} a_{25} - a_1 a_{15} a_{22} a_{25} + a_3^2 a_{23} a_{25} +$$
$$2a_3 a_4 a_{23} a_{25} + a_4^2 a_{23} a_{25} - a_1 a_9 a_{23} a_{25} - a_1 a_{10} a_{23} a_{25} -$$
$$a_1 a_{11} a_{23} a_{25} - a_1 a_{12} a_{23} a_{25}$$

$$r_4 = 2a_2 a_7 a_8 + a_8^2 a_9 + a_8^2 a_{10} + a_8^2 a_{11} + a_8^2 a_{12} + 2a_7 a_8 a_{13} +$$
$$2a_7 a_8 a_{14} + 2a_7 a_8 a_{15} - 2a_5 a_8 a_{16} - 2a_6 a_8 a_{16} - 2a_5 a_8 a_{17} -$$
$$2a_6 a_8 a_{17} - 2a_5 a_8 a_{18} - 2a_6 a_8 a_{18} - 2a_5 a_7 a_{19} - 2a_6 a_7 a_{19} -$$
$$2a_3 a_8 a_{19} - 2a_4 a_8 a_{19} + 2a_2 a_{16} a_{19} + 2a_2 a_{17} a_{19} + 2a_2 a_{18} a_{19} +$$
$$a_1 a_{19}^2 - 2a_5 a_7 a_{20} - 2a_6 a_7 a_{20} - 2a_3 a_8 a_{20} - 2a_4 a_8 a_{20} +$$
$$2a_2 a_{16} a_{20} + 2a_2 a_{17} a_{20} + 2a_2 a_{18} a_{20} + 2a_1 a_{19} a_{20} + a_1 a_{20}^2 -$$
$$a_2^2 a_{21} + a_5^2 a_{21} + 2a_5 a_6 a_{21} + a_6^2 a_{21} - a_2 a_{13} a_{21} - a_2 a_{14} a_{21} -$$
$$a_2 a_{15} a_{21} - a_2^2 a_{22} + a_5^2 a_{22} + 2a_5 a_6 a_{22} + a_6^2 a_{22} - a_2 a_{13} a_{22} -$$
$$a_2 a_{14} a_{22} - a_2 a_{15} a_{22} - a_1 a_2 a_{23} + 2a_3 a_5 a_{23} + 2a_4 a_5 a_{23} +$$
$$2a_3 a_6 a_{23} + 2a_4 a_6 a_{23} - a_2 a_9 a_{23} - a_2 a_{10} a_{23} - a_2 a_{11} a_{23} -$$
$$a_2 a_{12} a_{23} - a_1 a_{13} a_{23} - a_1 a_{14} a_{23} - a_1 a_{15} a_{23} - a_2 a_8^2 a_{27} -$$
$$a_8^2 a_{13} a_{27} - a_8^2 a_{14} a_{27} - a_8^2 a_{15} a_{27} + 2a_5 a_8 a_{19} a_{27} + 2a_6 a_8 a_{19} a_{27} -$$
$$a_2 a_{19}^2 a_{27} + 2a_5 a_8 a_{20} a_{27} + 2a_6 a_8 a_{20} a_{27} - 2a_2 a_{19} a_{20} a_{27} -$$
$$a_2 a_{20}^2 a_{27} + a_2^2 a_{23} a_{27} - a_5^2 a_{23} a_{27} - 2a_5 a_6 a_{23} a_{27} - a_6^2 a_{23} a_{27} +$$
$$a_2 a_{13} a_{23} a_{27} + a_2 a_{14} a_{23} a_{27} + a_2 a_{15} a_{23} a_{27}$$

(54)

$g_0 = r_1$, $g_6 = r_3$

$g_2 = a_2 a_7^2 + 2a_7 a_8 a_9 + 2a_7 a_8 a_{10} + 2a_7 a_8 a_{11} + 2a_7 a_8 a_{12} +$
$a_7^2 a_{13} + a_7^2 a_{14} + a_7^2 a_{15} - 2a_5 a_7 a_{16} - 2a_6 a_7 a_{16} - 2a_3 a_8 a_{16} -$
$2a_4 a_8 a_{16} + 2a_2 a_{16}^2 - 2a_5 a_7 a_{17} - 2a_6 a_7 a_{17} - 2a_3 a_8 a_{17} -$
$2a_4 a_8 a_{17} + 2a_2 a_{16} a_{17} + 2a_2 a_{17}^2 - 2a_5 a_7 a_{18} - 2a_6 a_7 a_{18} -$
$2a_3 a_8 a_{18} - 2a_4 a_8 a_{18} + 2a_2 a_{16} a_{18} + 2a_2 a_{17} a_{18} + a_2 a_{18}^2 -$
$2a_3 a_7 a_{19} - 2a_4 a_7 a_{19} + 2a_1 a_{16} a_{19} + 2a_1 a_{17} a_{19} + 2a_1 a_{18} a_{19} -$
$2a_3 a_7 a_{20} - 2a_4 a_7 a_{20} + 2a_1 a_{16} a_{20} + 2a_1 a_{17} a_{20} + 2a_1 a_{18} a_{20} -$
$a_1 a_2 a_{21} + 2a_3 a_5 a_{21} + 2a_4 a_5 a_{21} + 2a_3 a_6 a_{21} + 2a_4 a_6 a_{21} -$
$a_2 a_9 a_{21} - a_2 a_{10} a_{21} - a_2 a_{11} a_{21} - a_2 a_{12} a_{21} - a_1 a_{13} a_{21} -$
$a_1 a_{14} a_{21} - a_1 a_{15} a_{21} - a_1 a_2 a_{22} + 2a_3 a_5 a_{22} + 2a_4 a_5 a_{22} +$
$2a_3 a_6 a_{22} + 2a_4 a_6 a_{22} - a_2 a_9 a_{22} - a_2 a_{10} a_{22} - a_2 a_{11} a_{22} -$
$a_2 a_{12} a_{22} - a_1 a_{13} a_{22} - a_1 a_{14} a_{22} - a_1 a_{15} a_{22} + a_3^2 a_{23} +$
$2a_3 a_4 a_{23} + a_4^2 a_{23} - a_1 a_9 a_{23} - a_1 a_{10} a_{23} - a_1 a_{11} a_{23} - a_1 a_{12} a_{23}$

$g_4 = 2a_2 a_7 a_8 + a_8^2 a_9 + a_8^2 a_{10} + a_8^2 a_{11} + a_8^2 a_{12} + 2a_7 a_8 a_{13} +$
$2a_7 a_8 a_{14} + 2a_7 a_8 a_{15} - 2a_5 a_8 a_{16} - 2a_6 a_8 a_{16} -$
$2a_5 a_8 a_{17} - 2a_6 a_8 a_{17} - 2a_5 a_8 a_{18} - 2a_6 a_8 a_{18} - 2a_5 a_7 a_{19} -$
$2a_6 a_7 a_{19} - 2a_3 a_8 a_{19} - 2a_4 a_8 a_{19} + 2a_2 a_{16} a_{19} +$
$2a_2 a_{17} a_{19} + 2a_2 a_{18} a_{19} + a_1 a_{19}^2 - 2a_5 a_7 a_{20} - 2a_6 a_7 a_{20} -$
$2a_3 a_8 a_{20} - 2a_4 a_8 a_{20} + 2a_2 a_{16} a_{20} + 2a_2 a_{17} a_{20} +$
$2a_2 a_{18} a_{20} + 2a_1 a_{19} a_{20} + a_1 a_{20}^2 - a_2^2 a_{21} + a_5^2 a_{21} +$
$2a_5 a_6 a_{21} + a_6^2 a_{21} - a_2 a_{13} a_{21} - a_2 a_{14} a_{21} - a_2 a_{15} a_{21} - a_2^2 a_{22} +$
$a_5^2 a_{22} + 2a_5 a_6 a_{22} + a_6^2 a_{22} - a_2 a_{13} a_{22} - a_2 a_{14} a_{22} - a_2 a_{15} a_{22} -$
$a_1 a_2 a_{23} + 2a_3 a_5 a_{23} + 2a_4 a_5 a_{23} + 2a_3 a_6 a_{23} + 2a_4 a_6 a_{23} -$
$a_2 a_9 a_{23} - a_2 a_{10} a_{23} - a_2 a_{11} a_{23} - a_2 a_{12} a_{23} - a_1 a_{13} a_{23} -$
$a_1 a_{14} a_{23} - a_1 a_{15} a_{23}$

$\qquad\qquad (55)$

$y_5 = a_7^2 a_{24} - a_1 a_{21} a_{24} - a_1 a_{22} a_{24} - 2a_7 a_8 a_{24} a_{25} + a_2 a_{21} a_{24} a_{25} +$
$a_2 a_{22} a_{24} a_{25} + a_1 a_{23} a_{24} a_{25} + a_8^2 a_{24} a_{25}^2 - a_2 a_{23} a_{24} a_{25}^2$

$y_6 = a_7^2 a_{26} - a_1 a_{21} a_{26} - a_1 a_{22} a_{26} - 2a_7 a_8 a_{26} a_{27} +$
$a_2 a_{21} a_{26} a_{27} + a_2 a_{22} a_{26} a_{27} + a_1 a_{23} a_{26} a_{27} + a_8^2 a_{26} a_{27}^2 - a_2 a_{23} a_{26} a_{27}^2$

$J_0 = \dfrac{a_7^2 a_{24} - a_1 a_{21} a_{24} - a_1 a_{22} a_{24}}{a_{25}} - \dfrac{r_1 y_5}{a_{25} y_2} +$

$\dfrac{a_7^2 a_{26} - a_1 a_{21} a_{26} - a_1 a_{22} a_{26}}{a_{27}} - \dfrac{r_1 y_6}{a_{27} y_4}$

$\qquad\qquad (56)$

$J_2 = \dfrac{-a_7^2 a_{24} + a_1 a_{21} a_{24} + a_1 a_{22} a_{24} + 2a_7 a_8 a_{24} a_{25} -}{a_{25}^2}$
$\quad\quad \dfrac{a_2 a_{21} a_{24} a_{25} - a_2 a_{22} a_{24} a_{25} - a_1 a_{23} a_{24} a_{25}}{} -$

$\dfrac{r_3 y_5}{a_{25}^2 y_2} +$

$a_8^2 a_{26} - a_2 a_{23} a_{26} - \dfrac{r_4 y_6}{y_4}$

$J_4 = -\dfrac{r_2 y_5}{y_2} - \dfrac{r_2 y_6}{y_4}$

$y_7 = -a_3 a_7 a_{24} - a_4 a_7 a_{24} + a_1 a_{16} a_{24} + a_1 a_{17} a_{24} + a_1 a_{18} a_{24} +$
$a_5 a_7 a_{24} a_{25} + a_6 a_7 a_{24} a_{25} + a_3 a_8 a_{24} a_{25} + a_4 a_8 a_{24} a_{25} -$
$a_2 a_{16} a_{24} a_{25} - a_2 a_{17} a_{24} a_{25} - a_2 a_{18} a_{24} a_{25} - a_1 a_{19} a_{24} a_{25} -$
$a_1 a_{20} a_{24} a_{25} - a_5 a_8 a_{24} a_{25}^2 - a_6 a_8 a_{24} a_{25}^2 + a_2 a_{19} a_{24} a_{25}^2 + a_2 a_{20} a_{24} a_{25}^2$

$y_8 = -a_3 a_7 a_{26} - a_4 a_7 a_{26} + a_1 a_{16} a_{26} + a_1 a_{17} a_{26} + a_1 a_{18} a_{26} +$
$a_5 a_7 a_{26} a_{27} + a_6 a_7 a_{26} a_{27} + a_3 a_8 a_{26} a_{27} + a_4 a_8 a_{26} a_{27} -$
$a_2 a_{16} a_{26} a_{27} - a_2 a_{17} a_{26} a_{27} - a_2 a_{18} a_{26} a_{27} - a_1 a_{19} a_{26} a_{27} -$
$a_1 a_{20} a_{26} a_{27} - a_5 a_8 a_{26} a_{27}^2 - a_6 a_8 a_{26} a_{27}^2 + a_2 a_{19} a_{26} a_{27}^2 + a_2 a_{20} a_{26} a_{27}^2$

$r_5 = a_3 a_7 a_{24} + a_4 a_7 a_{24} - a_1 a_{16} a_{24} - a_1 a_{17} a_{24} - a_1 a_{18} a_{24} -$
$a_5 a_7 a_{24} a_{25} - a_6 a_7 a_{24} a_{25} - a_3 a_8 a_{24} a_{25} - a_4 a_8 a_{24} a_{25} +$
$a_2 a_{16} a_{24} a_{25} + a_2 a_{17} a_{24} a_{25} + a_2 a_{18} a_{24} a_{25} + a_1 a_{19} a_{24} a_{25} +$
$a_1 a_{20} a_{24} a_{25}$

$R_0 = \dfrac{-a_3 a_7 a_{24} - a_4 a_7 a_{24} + a_1 a_{16} a_{24} + a_1 a_{17} a_{24} + a_1 a_{18} a_{24}}{a_{25}} -$

$\dfrac{r_1 y_7}{a_{25} y_2} +$

$\dfrac{-a_3 a_7 a_{26} - a_4 a_7 a_{26} + a_1 a_{16} a_{26} + a_1 a_{17} a_{26} + a_1 a_{18} a_{26}}{a_{27}} -$

$\dfrac{r_1 y_8}{a_{27} y_4}$

$\qquad\qquad (57)$

$R_2 = \dfrac{r_5}{a_{25}^2} - \dfrac{r_3 y_7}{a_{25}^2 y_2} - a_5 a_8 a_{26} - a_6 a_8 a_{26} + a_2 a_{19} a_{26} + a_2 a_{20} a_{26} -$

$\dfrac{r_4 y_8}{y_4}$

$R_4 = -\dfrac{r_2 y_7}{y_2} - \dfrac{r_2 y_8}{y_4}$

$a_1 = A_{11} \alpha^2$, $a_2 = I_0$, $a_3 = B_{11} \alpha^3$, $a_4 = -C_{11} \alpha^3$,
$a_5 = I_1 \alpha$, $a_6 = -I_3 \alpha$, $a_7 = C_{11} \alpha^2$
$a_8 = I_3$, $a_9 = -2E_{11} \alpha^4$, $a_{10} = H_{11} \alpha^4$,
$a_{11} = D_{11} \alpha^4$, $a_{12} = A_{55} \alpha^2$, $a_{13} = I_2 \alpha^2$, $a_{14} = -2I_4 \alpha^2$
$a_{15} = I_5 \alpha^2$, $a_{16} = -H_{11} \alpha^3$, $a_{17} = E_{11} \alpha^3$,
$a_{18} = -A_{55} \alpha$, $a_{19} = I_4 \alpha$, $a_{20} = -I_5 \alpha$
$a_{21} = H_{11} \alpha^2$, $a_{22} = A_{55}$, $a_{23} = I_5$,
$a_{24} = P(V_0 \alpha + \omega)$, $a_{25} = (V_0 \alpha + \omega)^2$
$a_{26} = P(\omega - V_0 \alpha)$, $a_{27} = (\omega - V_0 \alpha)^2$

$\qquad\qquad (58)$

References

[1] Eghbali, M., Hosseini, S.A. & Hamidi, B.A., 2022. Mantari's higher-order shear deformation theory of sandwich beam with cntrc face layers with porous core under thermal loading. *International Journal of Structural Stability and Dynamics*, pp.2250181.

[2] Eghbali, M. & Hosseini, S.A., 2022. Influences of magnetic environment and two moving loads on lateral and axial displacement of sandwich graphene-reinforced copper-based composite beams with soft porous core. *Journal of Vibration and Control*, pp.10775463221135030.

[3] Eghbali, M., Hosseini, S.A. & Pourseifi, M., 2022. Free transverse vibrations analysis of size-dependent cracked piezoelectric nano-beam based on the strain gradient theory under mechanic-electro forces. *Engineering Analysis with Boundary Elements, 143*, pp.606-612.

[4] Zhao, Y., Qin, B., Wang, Q. & Liang, X., 2022. A unified jacobi–ritz approach for the fgp annular plate with arbitrary boundary conditions based on a higher-order shear deformation theory. *Journal of Vibration and Control*, pp.10775463211072677.

[5] Xiao, C., Zhang, G., Yu, Y., Mo, Y. & Mohammadi, R., 2022. Nonlinear vibration analysis of the nanobeams subjected to magneto-electro-thermal loading based on a novel hsdt. *Waves in Random and Complex Media*, pp.1-20.

[6] Ramezani, M., Rezaiee-Pajand, M. & Tornabene, F., 2022. Nonlinear thermomechanical analysis of cntrc cylindrical shells using hsdt enriched by zig-zag and polyconvex strain cover functions. *Thin-Walled Structures, 172*, pp.108918.

[7] Melaibari, A., Daikh, A.A., Basha, M., Abdalla, A.W., Othman, R., Almitani, K.H., Hamed, M.A., Abdelrahman, A. & Eltaher, M.A., 2022. Free vibration of fg-cntrcs nano-plates/shells with temperature-dependent properties. *Mathematics, 10* (4), pp.583.

[8] Van Quyen, N., Van Thanh, N., Quan, T.Q. & Duc, N.D., 2021. Nonlinear forced vibration of sandwich cylindrical panel with negative poisson's ratio auxetic honeycombs core and cntrc face sheets. *Thin-Walled Structures, 162*, pp.107571.

[9] Hosseini, S.A., Rahmani, O. & Bayat, S., 2021. Thermal effect on forced vibration analysis of fg nanobeam subjected to moving load by laplace transform method. *Mechanics Based Design of Structures and Machines*, pp.1-20.

[10] Dat, N.D., Quan, T.Q., Mahesh, V. & Duc, N.D., 2020. Analytical solutions for nonlinear magneto-electro-elastic vibration of smart sandwich plate with carbon nanotube reinforced nanocomposite core in hygrothermal environment. *International Journal of Mechanical Sciences, 186*, pp.105906.

[11] Cheshmeh, E., Karbon, M., Eyvazian, A., Jung, D.W., Habibi, M. & Safarpour, M., 2020. Buckling and vibration analysis of fg-cntrc plate subjected to thermo-mechanical load based on higher order shear deformation theory. *Mechanics Based Design of Structures and Machines*, pp.1-24.

[12] Bouazza, M. & Zenkour, A.M., 2020. Vibration of carbon nanotube-reinforced plates via refined nth-higher-order theory. *Archive of Applied Mechanics, 90* (8), pp.1755-1769.

[13] Nematollahi, M.S. & Mohammadi, H., 2019. Geometrically nonlinear vibration analysis of sandwich nanoplates based on higher-order nonlocal strain gradient theory. *International Journal of Mechanical Sciences, 156*, pp.31-45.

[14] Civalek, Ö., 2008. Analysis of thick rectangular plates with symmetric cross-ply laminates based on first-order shear deformation theory. *Journal of Composite Materials, 42* (26), pp.2853-2867.

[15] Akgöz, B. & Civalek, Ö., 2018. Vibrational characteristics of embedded microbeams lying on a two-parameter elastic foundation in thermal environment. *Composites Part B: Engineering, 150*, pp.68-77.

[16] Demir, C., Mercan, K., Numanoglu, H.M. & Civalek, O., 2018. Bending response of nanobeams resting on elastic foundation. *Journal of Applied and Computational Mechanics, 4* (2), pp.105-114.

[17] Daikh, A.A., Houari, M.S.A., Belarbi, M.O., Chakraverty, S. & Eltaher, M.A., 2022. Analysis of axially temperature-dependent functionally graded carbon nanotube reinforced composite plates.

Engineering with Computers, 38 (3)**,** pp.2533-2554.

[18] Melaibari, A., Daikh, A.A., Basha, M., Wagih, A., Othman, R., Almitani, K.H., Hamed, M.A., Abdelrahman, A. & Eltaher, M.A., 2022. A dynamic analysis of randomly oriented functionally graded carbon nanotubes/fiber-reinforced composite laminated shells with different geometries. *Mathematics, 10* (3)**,** pp.408.

[19] Eltaher, M.A., Almalki, T., Almitani, K. & Ahmed, K., Participation factor and vibration of carbon nanotube with vacancies. Journal of Nano Research, 2019. Trans Tech Publ, 158-174.

[20] Mohamed, N., Eltaher, M.A., Mohamed, S.A. & Seddek, L.F., 2019. Energy equivalent model in analysis of postbuckling of imperfect carbon nanotubes resting on nonlinear elastic foundation. *Structural Engineering and Mechanics, An Int'l Journal, 70* (6)**,** pp.737-750.

[21] Abdelrahman, A.A., Esen, I., Daikh, A.A. & Eltaher, M.A., 2021. Dynamic analysis of fg nanobeam reinforced by carbon nanotubes and resting on elastic foundation under moving load. *Mechanics Based Design of Structures and Machines***,** pp.1-24.

[22] Esen, I., Daikh, A.A. & Eltaher, M.A., 2021. Dynamic response of nonlocal strain gradient fg nanobeam reinforced by carbon nanotubes under moving point load. *The European Physical Journal Plus, 136* (4)**,** pp.1-22.

[23] Khadir, A.I., Daikh, A.A. & Eltaher, M.A., 2021. Novel four-unknowns quasi 3d theory for bending, buckling and free vibration of functionally graded carbon nanotubes reinforced composite laminated nanoplates. *Advances in nano research, 11* (6)**,** pp.621-640.

[24] Song, J., Karami, B., Shahsavari, D. & Civalek, Ö., 2021. Wave dispersion characteristics of graphene reinforced nanocomposite curved viscoelastic panels. *Composite Structures, 277***,** pp.114648.

[25] Huang, Y., Karami, B., Shahsavari, D. & Tounsi, A., 2021. Static stability analysis of carbon nanotube reinforced polymeric composite doubly curved micro-shell panels. *Archives of Civil and Mechanical Engineering, 21* (4)**,** pp.1-15.

[26] Karami, B. & Shahsavari, D., 2020. On the forced resonant vibration analysis of functionally graded polymer composite doubly-curved nanoshells reinforced with graphene-nanoplatelets. *Computer Methods in Applied Mechanics and Engineering, 359***,** pp.112767.

[27] Karami, B., Shahsavari, D., Janghorban, M. & Li, L., 2019. Elastic guided waves in fully-clamped functionally graded carbon nanotube-reinforced composite plates. *Materials Research Express, 6* (9)**,** pp.0950a9.

[28] Ke, L.-L., Yang, J. & Kitipornchai, S., 2010. Nonlinear free vibration of functionally graded carbon nanotube-reinforced composite beams. *Composite Structures, 92* (3)**,** pp.676-683.

[29] Shen, H.-S. & Xiang, Y., 2013. Nonlinear analysis of nanotube-reinforced composite beams resting on elastic foundations in thermal environments. *Engineering Structures, 56***,** pp.698-708.

[30] Ansari, R., Torabi, J. & Hasrati, E., 2018. Axisymmetric nonlinear vibration analysis of sandwich annular plates with fg-cntrc face sheets based on the higher-order shear deformation plate theory. *Aerospace Science and Technology, 77***,** pp.306-319.

[31] Ansari, R., Hasrati, E. & Torabi, J., 2019. Nonlinear vibration response of higher-order shear deformable fg-cntrc conical shells. *Composite Structures, 222***,** pp.110906.

[32] Wattanasakulpong, N. & Ungbhakorn, V., 2013. Analytical solutions for bending, buckling and vibration responses of carbon nanotube-reinforced composite beams resting on elastic foundation. *Computational Materials Science, 71***,** pp.201-208.

[33] Mantari, J., Bonilla, E. & Soares, C.G., 2014. A new tangential-exponential higher order shear deformation theory for advanced composite plates. *Composites Part B: Engineering, 60***,** pp.319-328.

[34] Eghbali, M., Hosseini, S.A. & Rahmani, O., 2021. Free vibration of axially functionally graded nanobeam with an attached mass based on nonlocal strain gradient theory via new adm numerical method. *Amirkabir Journal of Mechanical Engineering, 53* (Issue 2 (Special Issue))**,** pp.8-8.

[35] Hosseini, S. & Rahmani, O., 2017. Exact solution for axial and transverse dynamic response of functionally graded nanobeam under moving constant load based on nonlocal elasticity theory. *Meccanica, 52* (6)**,** pp.1441-1457.